NMR Verification of Helical Conformations of Phycocyanobilin in Organic Solvents

by **Bernd Knipp, Martin Müller, Nils Metzler-Nolte, Teodor S. Balaban, Silvia E. Braslavsky*,** and **Kurt Schaffner**

Max-Planck-Institut für Strahlenchemie, Postfach 10 13 65, D-45413 Mülheim an der Ruhr

Dedicated to Prof. *Günther Schenck* on the occasion of his 85th birthday

Selective NMR decoupling and nuclear *Overhauser* effect (NOE) experiments with phycocyanobilin (PCB) show proton-proton interactions between the terminal rings A and D, *viz.* the chiral C(2) methine center and the ethyl substituent at C(18), as a result of the helical conformation of this open-chain tetrapyrrole in solution. Quantitative NOE measurements and a combination of force-field and semiempirical calculations (FSC) afford inter-proton distances across the helical gap of 4.2–4.6 (NOE) and 3.2–4.2 A° (FSC). The NOE and FSC, in conjunction with a qualitative evaluation of the steric interactions in the two optimized helices, suggest furthermore that, in solution, the helix **M** is somewhat more stable than **P**. The coexistence of at least two diastereoisomers is corroborated also by the circular dichroism (CD) spectra of PCB in MeOH/EtOH which point to a temperature-dependent equilibrium in solution, and by a considerable increase of this CD upon changing the solvent from the achiral alcohols to ethyl (–)-(*S*)-lactate which reflects a selective solvent-induced CD differentiating between diastereoisomers.

1. Introduction. – Phycocyanobilin (PCB[1]); *Fig. 1*) is the chromophore of the antenna pigment phycocyanin, a chromoprotein present in several algae, *e.g.*, *Spirulina geitleri*, from which it can be readily isolated [1–3]. The chiral center C(2) in ring A of native PCB predominantly possesses the (*R*)-configuration [4][5].

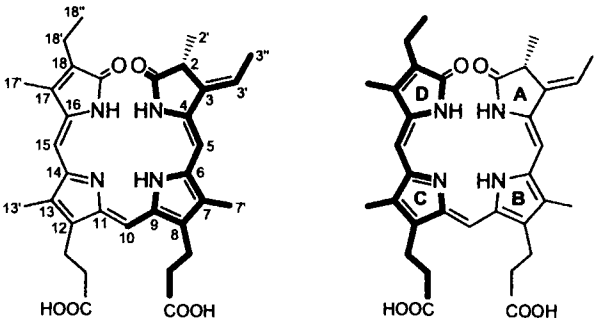

Fig. 1. *Helices* **M** *and* **P** *of (2R)-phycocyanobilin* (PCB)

[1]) Abbreviations: BV(E), biliverdin (dimethyl ester). FSC, force field and semiempirical calculations. ISPA, isolated spin pair approximation. NOE, nuclear *Overhauser* effect. NOESY, nuclear *Overhauser* enhanced spectroscopy. PCB(E), phycocyanobilin (dimethyl ester).

So far, the conformation of PCB has not been investigated as thoroughly as that of the related biliverdin (BV). In particular, spectroscopic studies have indicated that biliverdin dimethyl ester (BVE) is mostly in an (all-*Z*,all-*syn*)-conformation in solution as well as in the crystal [6–11]. Application of COSY and two-dimensional spin-locked nuclear *Overhauser* effects (NOE) in 500-MHz ^{1}H-NMR spectra of PCB in (D_5)pyridine exhibited proton cross-peaks between the methine groups and the neighboring alkyl substituents on the pyrrole rings [12], which indicates that the (all-*Z*,all-*syn*)-conformation predominates similarly to the case of BVE [8][10–13].

Investigations using racemic mixtures of chiral BVs [7][14], phycocyanobilin dimethyl ester (PCBE) [5][15] and a chiral derivative [3], and optically active BVs [14][16] also demonstrated that in solution helical species of type **M** and **P**[2]) are coexistent for all these compounds. Additional support has come forth from the fluorescence and fluorescence excitation spectra of PCBE in MeOH/Et_3N 10:1 which indicate that, in analogy to BVE, PCBE in solution is present in two families of conformers, one helical and the other one stretched [3].

Should PCB in solution exist in a cyclic conformation, the methylene protons at C(18′) of ring D would give rise to a typical NMR spectrum, the intrinsic diastereotopic characteristics of which are enhanced by through-space interaction with the chiral ring A. Furthermore, NOEs between the substituents on the terminal rings may be observed under favorable conditions. One- and two-dimensional ^{1}H-NMR studies in several solvents, as reported in this paper, establish such interactions between the terminal rings in PCB and in PCBE. CD Measurements of PCB in various solvents confirm the presence of the diastereoisomers in solution.

2. Results and Discussion. – 2.1. *^{1}H-NMR Data.* Using a combination of one- and two-dimensional NMR spectroscopy, an unambiguous assignment of all resonances in PCB was achieved. The 400- and 500-MHz ^{1}H-NMR spectra (*Fig. 2,c*) show a *m* for the diastereotopic CH_2(18′) protons at δ 2.49, in accord with the data reported earlier [12]. Contrary to the literature claim [12], however, the signal splitting cannot be due to homoallylic coupling of CH_2(18′) to Me(17′), since the latter protons appear as a sharp *s* at δ 2.09.

A first hint to the presence of more than one conformation in solution comes from a close inspection of the CH_2(18′) ^{1}H-NMR signal at δ 2.49, which in pyridine has the appearance of a *sept*. The *AB* spin system for CH_2(18′) is unequivocally established by selective decoupling of the Me(18″) protons at δ 1.25 (*Fig. 2,b*) and the C(18′) protons at δ 2.49 (*Fig. 2,a*). The *AB* spin system arises from the fact that the CH_2(18′) protons are diastereotopic. Two causes for this need to be considered: the mere existence of a stereogenic centre at C(2) (even if it were racemic), and the coexistence of two helical forms, **M** and **P**, which are different in energy and hence differently populated. If protons *A* and *B* at C(18′), on the one hand, have different chemical shifts in the two conformations, an *AB* system results even if the two conformers are in fast exchange. The chemical-shift difference $\Delta\delta_{AB}$ is then a function of the shift difference in each of the helical forms **M** and **P** as well as of the equilibrium constant $K = [\mathbf{M}]/[\mathbf{P}]$. Cooling the sample, on the other hand, should increase the population difference, changing the *AB* towards an

[2]) Helical conformers of open-chain tetrapyrroles are often referred to as 'cyclic' arrangements.

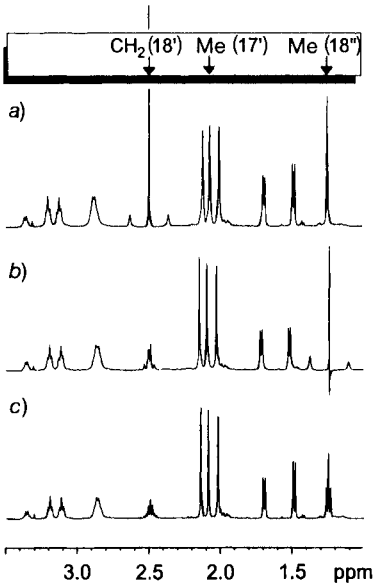

Fig. 2. *500-MHz ^{1}H-NMR Spectra of PCB in (D_5)pyridine* (δ 1.0–3.5): a) *CH_2(18') protons* (δ 2.49) *decoupled*, b) *Me(18") protons* (δ 1.25) *decoupled; and* c) *not decoupled*

AX spin system. Throughout the temperature range (233–348 K) available for our NMR experiments, however, there was no significant spectral change. Given the small energy difference between the forms **M** and **P**, as calculated by force-field calculations (FSC; see below), this result is not unexpected. Changing the solvent could also alter *K*, and indeed, the *AB* system changed to A_2 upon adding CD_2Cl_2 or $CDCl_3$ to (D_5)pyridine in increasing concentrations (*Table 1, a*).

Table 1. *Signal Multiplicities of the Methylene Protons CH_2(18') (δ 2.49–2.27) of PCB and PCBE in Various Solvent Mixtures, and Results of Selective Decoupling of the Me(18") Protons in the Range of δ 1.09–1.25*

Solvent		Normal signal	δ [ppm]	Decoupled signal	$\Delta\delta$ [ppm]
a) PCB	(D_5)pyridine	*m*	2.49	*AB* system	0.010
	$CDCl_3$/(D_5)pyridine 1:1	*m*	2.43	*AB* system	0.0102
	$CDCl_3$/(D_5)pyridine 2:1	*m*	2.37	broad *s*	n.d.[a])
	$CDCl_3$/(D_5)pyridine 3:1	split *q*	2.32	broad *s*	n.d.[a])
	$CDCl_3$/(D_5)pyridine 10:1	split *q*	2.23	broad *s*	n.d.[a])
	CD_2Cl_2/(D_5)pyridine 3:1	split *q*	2.34	broad *s*	n.d.[a])
	CD_2Cl_2/(D_5)pyridine 10:1	*q*	2.32	–	–
	(D_8)THF	*q*	2.27	–	–
	CD_3OD + 1% Et_3N	*q*	2.29	–	–
b) PCBE	(D_5)pyridine	*m*	2.48	*AB* system	0.012
	$CDCl_3$	*q*	2.31	–	–
	CD_3OD	*q*	2.29	–	–
	CD_3OD + 1% Et_3N	*q*	2.28	–	–

[a]) Not detected.

The *AB* system turning to A_2 is observed also with PCBE (*Table 1, b*). This rules out deprotonation of the propanoic-acid side chains in PCB when in pyridine as solvent, with negative charges increasing the energy difference between the two helical conformations as the cause for this spectral change in PCB[3]).

Spectra of PCB and PCBE in CD_3OD solution with added Et_3N, instead of in (D_5)pyridine, were almost identical to spectra taken in neat CD_3OD. It is, therefore, not the basicity of the solvent alone which is responsible for the *AB* spin system, *e.g.*, by stabilizing H-bridges of the amide protons. Rather, pyridine may play a decisive role in rendering the environment of $CH_2(18')$ more unsymmetrical by π stacking to ring D. Attractive forces between pairs of electron-rich and electron-poor aromatic systems can be considerable in energy and have been exploited for the self-assembly of large organic molecules [18]. For PCB under the conditions used in this study, however, the effect appears to be quite small energetically. Although *Table 1, a*, shows that increasing amounts of pyridine do indeed lead to a more pronounced *AB* system, we were unable to detect cross-peaks between pyridine and PCB in a nuclear-*Overhauser*-enhanced spectrum (NOESY) of a pyridine solution.

A word of caution is appropriate with regard to the coexistence of two diastereoisomeric, and, therefore, energetically different, helical forms in solution: chemical shifts are generally solvent-dependent, and the *AB*-to-A_2 transition could simply be induced by chance. It is pertinent in this connection to note that intermolecular interactions cannot cause the effect, since the spectra are independent of concentration in the range 1.7–24 mM in (D_5)pyridine, *i.e.*, PCB is monomeric under the conditions the *AB* splitting of the $CH_2(18')$ protons is observed. It is difficult, consequently, to determine the origin of this effect unambiguously on the basis of the above data alone.

There remained the possibility to analyze more thoroughly the conformation of PCB by NOE and NOESY measurements. After careful optimization of the experimental parameters, we were indeed able to detect transannular NOE enhancements by steady-state 1D difference NOE and 2D NOESY experiments. Extraction of NOE enhancements from appropriately processed columns in a 2D NOESY gave absolute $^1H,^1H$-NOE enhancements between H–C(2) (δ 3.35) and Me(18″) (δ 1.25) (in **M**) as well as Me(2′) (δ 1.49) and $CH_2(18')$ (δ 2.49) (in **P**) of 0.04 and 0.02%, respectively (in (D_5)pyridine, 400 ms mixing time). As small as this difference between **M** and **P** appears in absolute terms, it may still be significant, given the similarity in structural parameters underlying the two NOEs.

A more quantitative interpretation of the 2D NOESY spectrum was carried out subsequently. The following $^1H,^1H$-NOEs were clearly resolved and could be accurately integrated: Me(2′) to $CH_2(18')$ (see *Fig. 3*: interaction **I**, both directions), H–C(2) to $CH_2(18')$ (interaction **II**), and H–C(2) to Me(18′) (interaction **III**). These NOEs establish unambiguously the presence of *both* helical forms, **P** and **M** (*cf.* the calculated structures in *Fig. 3, a* and *b*) in solution, since **I** will only occur in **P** and **II** and **III** only in **M**. Within the framework of the isolated spin pair approximation (ISPA), we were thus able to calculate inter-proton distances across the helical gap by using distances H–C(2) to Me(3″) of 2.9 Å and H–C(5) to Me(7′) of 2.55 Å as internal standards [19][20]. For

[3]) In earlier studies at 90 MHz, similar observations were technically precluded [17].

Me groups, very fast internal rotation was assumed, and a mean distance was calculated according to the literature [21]. From these data, H,H distances Me(2′) to CH_2(18′), H–C(2) to CH_2(18′), and H–C(2) to Me(18″) were calculated to be 4.5, 4.2, and 4.6 Å, respectively. Of course, these distance calculations are a mere approximation since the observed NOEs are the result of time-averaged cross relaxation and total relaxation rates (Chapt. 5 in [19]), which is neglected in the ISPA approximation used here. Nevertheless, these values are comparable with the data from FSC (4.0, 3.2, and 4.2 Å for the distances between H-atoms as above and 4.0 Å for the O(1)–O(19) distance) and are also in agreement with the X-ray data of 2,3-dihydrobilins. In particular, 3,3,7,8,12,13,18-heptamethyl-17-ethyl-2,3-dihydrobilatriene-abc shows a helical pitch with an O(1)–O(19) distance of 3.47 Å and a puckering amplitude of 0.08 Å [22][23].

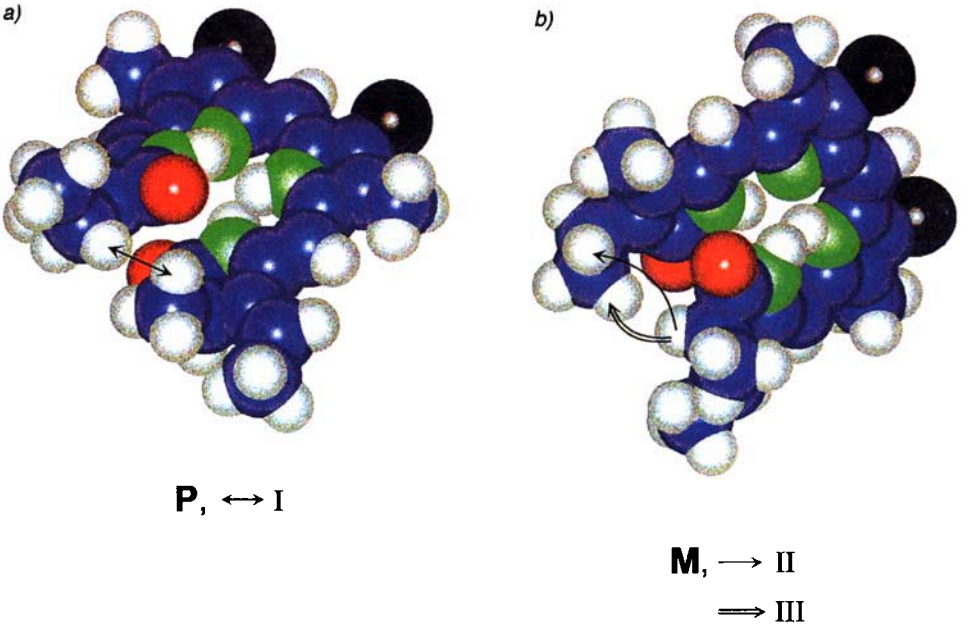

Fig. 3. *Calculated molecular structures of the helical (2*R*)-PCB, illustrating the NOE through-space interactions between* a) *the Me(2′) and CH_2(18′) protons* (in both directions) *in the helix* **P** (interaction **I**), *and* b) *the H–C(2) and CH_2(18′) protons* (interaction **II**) *and the H–C(2) and Me(18″) protons in the helix* **M** (interaction **III**). Violet spheres designate C-atoms, white H-atoms, red O-atoms, and green N-atoms. The black spheres stand for the propanoic-acid side chains.

The use of a relatively long mixing time in the NOESY was necessary to get sufficient NOE transfer for a good signal-to-noise ratio. Since PCB is a relatively small molecule, its overall correlation time for isotropic tumbling is expected to be no larger than 2 ns, resulting in an estimated error of 50% in our calculated distances [20]. Given these limitations and the complete neglect of inter-proton relaxation within ISPA, the agreement between the distances estimated by NMR and calculated by FSC is astonishingly good and, to some degree, possibly the result of fortuitous cancellation of errors. Nevertheless, PCB is a fairly rigid molecule with essentially two well-defined conformations

making it a well-suited object for NMR studies. Our findings demonstrate that partial structure determination even of small molecules with only a few NOEs in solution can be carried out in a quantitative way leading to reasonable results.

2.2. *Circular Dichroism.* The CD spectrum of PCB in MeOH/EtOH 1:4 at room temperature shows a relatively weak band at 650 nm (*Fig. 4*), red-shifted with respect to the UV/VIS absorption maximum at 610 nm. Upon lowering the temperature from + 20 to −160°, this CD shifts still farther to the red, and the amplitude increases about four times, which is compatible with a temperature-dependent equilibrium between diastereoisomers. In the presence of a chiral solvent such as ethyl (−)-(*S*)-lactate, PCB at room temperature exhibits a CD coincident in wavelength with that in the achiral alcohols at the same temperature, but four times more intense. We interpret this finding as a selective solvent-induced CD differentiating between diastereoisomers.

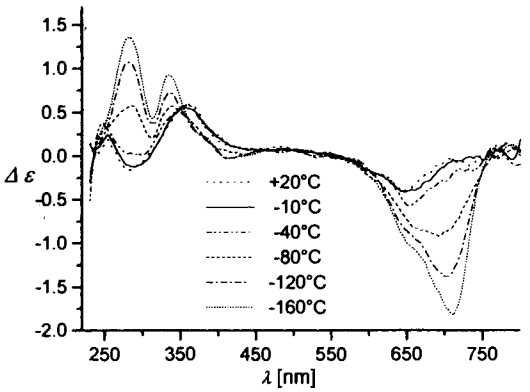

Fig. 4. *CD Spectra of PCB in MeOH/EtOH 1:4 in the temperature range of + 20 to −160°*

2.3. *Force-Field Calculations.* They were performed within the program package *Hyperchem*™ on an *IBM*-compatible personal computer (*Intel Pentium 586* processor, 64 KB RAM). The PCB molecule was assembled from initially minimized fragments such as a 1*H*-pyrrole ring, a 2*H*-pyrrole ring, and two maleic imides. A pyrromethene (= 11*H*-dipyrrin) was then formed by joining a 2-methylidene-2*H*-pyrrole with the 1*H*-pyrrole ring, and this was minimized by molecular mechanics with the MM + force field. The joining of the two maleic imides to the pyrromethene was then performed by means of methine bridges in two different conformations corresponding to the helices **M** and **P**. Slight adjustments of the torsion angles between the five-membered rings allowed for different start geometries. These were extensively minimized again by MM+. Only two final conformations were obtained, whether the starting geometry was **M** or **P**. These two conformers were then submitted to a geometry optimization within the semiempirical PM3 method [24].

This procedure allows for the calculation of *Mulliken* charges for each atom. The two final conformations differed slightly from those obtained by molecular mechanics alone, mainly in the torsion angles between the five-membered rings.

The propanoic-acid side chains were then added to the two structures, and another MM + optimization cycle was performed. No conformational search of the two flexible side chains was carried out, since the main concern was the overall geometry of the

tetrapyrrole moiety. The helical nature of this system was fully reproduced by the calculations as shown in *Fig. 3, a* and *b*. The final MM + geometries and also the energies were found to depend on the charge distribution obtained by the PM3 method. The dihedral angles between the rings show the typical torsion of an open-chain tetrapyrrole (*Table 2*).

Table 2. *Dihedral Angles* (deg) *of the Helices* **P** *and* **M** *of PCB Calculated from the FSC Data*

	P	**M**
C(3)–C(4)–C(5)–C(6)	0.88	–3.56
C(4)–C(5)–C(6)–C(7)	–16.07	12.6
C(8)–C(9)–C(10)–C(11)	–12.03	8.59
C(9)–C(10)–C(11)–C(12)	– 0.17	0.79
C(13)–C(14)–C(15)–C(16)	–18.9	27.63
C(14)–C(15)–C(16)–C(17)	– 0.41	0.10

Neither the slight energy preference of 0.6 kcal/mol for the helix **M** (51.93 kcal/mol) over **P** (52.53 kcal/mol), calculated by a combination of force field and semiempirical PM3 methods, nor the absolute NOE enhancements (0.04 *vs.* 0.02%) alone reliably suffice, within the precision of the methods involved, to identify **M** as the prevalent helix. However, the two arguments in favor of **M** concur with an estimate of the through-space steric interactions between the terminal rings A and D in the two optimized helical structures.

Experimental Part

Chemicals. CD_2Cl_2, (D_5)pyridine, $CDCl_3$, and (D_8)THF were purchased from *Sigma* (Deisenhofen, Germany). All solvents were of > 99% purity. PCB was isolated from commercially available *Spirulina geitleri* (*Winfried Behr*, Bonn) by methanolysis, protein separation, and HPLC separation [1–3]. PCBE was prepared as reported earlier [3]. Recrystallization from $CHCl_3$/MeOH/hexane afforded PCB in a purity of 97–99% [1], checked by anal. HPLC (*RP C-18 Nucleosil* 25 × 0.46 cm, MeCN/14 mM phosphate buffer soln., (pH 7.2) 28:72 (*v*/*v*) and by ^{1}H-NMR. In PCB and PCBE, the (*R*) enantiomers were predominant [5]. Both samples were used without further enantiomer separation.

^{1}H-NMR Measurements. Bruker-270-,-400-, and -500-MHz spectrometers; sat. solns. of PCB in 5-mm tubes, degassed by three freeze-pump-thaw cycles (cooling with liq. N_2); δ in ppm (referenced against residual ^{1}H signals in the deuterated solvents), *J* in Hz. Because of the solubility properties of PCB, it was necessary to use either neat (D_5)pyridine or mixtures of (D_5)pyridine and CD_2Cl_2 or $CDCl_3$, rather than neat CD_2Cl_2, $CDCl_3$, or (D_8)THF. ^{1}H-NMR of PCB (500 MHz, (D_5)pyridine): 7.25 (*s*, H–C(10)); 6.31 (*q*, *J* = 6.5, H–C(3′)); 6.07 (*s*, H–C(15)); 5.86 (*s*, H–(5)); 3.35 (*q*, *J* = 7.7, H–C(2)); 3.19 (*t*, *J* = 7.2, CH_2(12′)); 3.11 (*t*, *J* = 7.5, CH_2(8′)); 2.86 (unresolved *t*, CH_2(12″)); 2.85 (unresolved *t*, CH_2(8″); 2.49 (*m*, see text, CH_2(18′)); 2.14 (*s*, Me(13′)); 2.09 (*s*, Me(17′)); 2.02 (*s*, Me(7′)); 1.70 (*d*, *J* = 7.3, Me(3″)); 1.49 (*d*, *J* = 7.7, Me(2′)); 1.25 (*t*, *J* = 7.5, Me(18″)). The dynamic NMR measurements were performed in (D_5)pyridine/CD_2Cl_2 1:5, 1:10, and 1:20. A limiting factor for the lowest attainable temp. (233 K) was the pyridine content of the sample which caused an increase in viscosity and broadening of the otherwise sharp NMR signals. For selective decoupling experiments, the decoupler power was adjusted as low as possible. Complete decoupling under such conditions was confirmed when no spectral changes occurred in the decoupled signal upon a subsequent increase in decoupler power by 8 dB.

2D Spectra. They were typically run over the entire spectral range at 400 or 500 MHz with 1024 × 256 data points. The data were *Fourier* transformed after zero-filling in both dimensions and applying a matched cosine function. For NOESY spectra, several mixing times were tested and a value of 400 ms was found to give best results for the detection of the long-range NOEs.

Circular Dichroism. AVIV® model *62* (*ADS* spectrometer); in 1.0-cm quartz cuvettes; *ca.* $0.3 \cdot 10^{-4}$ M in MeOH/EtOH 1:4 from + 20 to –160° or in ethyl (–)-(*S*)-lactate at r.t.

We thank Professor Dr. *J. Buddrus, Gesellschaft zur Förderung der Spektrochemie und angewandten Spektroskopie e.V.*, Dortmund, and PD Dr. *W. Gärtner, MPI für Strahlenchemie*, for helpful discussions, and Professor Dr. *V. Buss* and Mr. *G. Rapp*, Gerhard-Mercator University, Duisburg, for support with the CD measurements.

REFERENCES

[1] W. Kufer, H. Scheer, *Hoppe-Seyler's Z. Physiol. Chem.* **1979**, *360*, 935.
[2] H. L. Crespi, U. Smith, J. J. Katz, *Biochemistry* **1968**, *7*, 2232 ; W. J. Cole, D. J. Chapman, H. W. Siegelmann, *ibid.* **1968**, *7*, 2929.
[3] S. E. Braslavsky, D. Schneider, K. Heihoff, S. Nonell, P. F. Aramendía, K. Schaffner, *J. Am. Chem. Soc.* **1991**, *113*, 7322.
[4] H. Brockmann, Jr., G. Knobloch, *Chem. Ber.* **1973**, *106*, 803.
[5] J. E. Bishop, J. O. Nagy, J. F. O'Connell, H. Rapoport, *J. Am. Chem. Soc.* **1991**, *113*, 8024.
[6] S. E. Braslavsky, A. R. Holzwarth, K. Schaffner, *Angew. Chem., Int. Ed. Engl.* **1983**, *22*, 656.
[7] J. Claret, O. Ibars, K. Lang, F. R. Trull, D. A. Ligthner, *Biochim. Biophys. Acta* **1995**, *1243*, 221.
[8] H. Lehner, S. E. Braslavsky, K. Schaffner, *Liebigs Ann. Chem.* **1978**, 1990; H. Falk, K. Grubmayr, E. Haslinger, T. Schlederer, K. Thirring, *Monatsh. Chem.* **1978**, *109*, 1451.
[9] K. Smit, J. Matysik, P. Hildebrandt, F. Mark, *J. Phys. Chem.* **1993**, *97*, 11887.
[10] H. Lehner, S. E. Braslavsky, K. Schaffner, *Angew. Chem., Int. Ed. Engl.* **1978**, *17*, 948; W. S. Sheldrick, *J. Chem. Soc., Perkin Trans. 2* **1976**, 1457.
[11] BVE Analogue: P. Nesvadba, D. Ngoc-Phan, F. Nydegger, A. E. Ferao, A. Gossauer, *Helv. Chim. Acta* **1994**, *77*, 1837.
[12] D. M. Arciero, J. L. Dallas, A. N. Glazer, *J. Biol. Chem.* **1988**, *263*, 18350.
[13] D. M. Arciero, D. A. Bryant, A. N. Glazer, *J. Biol. Chem.* **1988**, *263*, 18343.
[14] H. Lehner, W. Riemer, K. Schaffner, *Liebigs Ann. Chem.* **1979**, 1798; D. Krois, H. Lehner, *Monatsh. Chem.* **1986**, *117*, 1205; *ibid.* **1995**, *126*, 349; *J. Chem. Soc., Perkin Trans. 2* **1995**, 489.
[15] R. Micura, K. Grubmayr, *Enantiomer* **1996**, *1*, 106.
[16] S. E. Boiadjiev, D. T. Anstine, D. A. Lightner, *Tetrahedron Asym.* **1995**, *6*, 901.
[17] A. Gossauer, W. Hirsch, *Liebigs Ann. Chem.* **1974**, 1496; M. J. Terry, M. D. Maines, J. C. Lagarias, *J. Biol. Chem.* **1993**, *35*, 26099.
[18] D. B. Amabilino, J. F. Stoddart, *Chem. Rev.* **1995**, *95*, 2725.
[19] D. Neuhaus, M. Williamson, 'The Nuclear Overhauser Effect in Structural and Conformational Analysis', VCH, New York, 1989.
[20] G. C. K. Roberts, 'NMR of Macromolecules – A Practical Approach', Oxford University Press, Oxford, 1993, Vol. 134.
[21] A. M. Gronenborn, G. M. Clore, *Progr. Nucl. Magn. Reson. Spectrosc.* **1985**, *17*, 1; T. M. G. Koning, R. Boelens, R. J. Kaptein, *J. Magn. Reson.* **1990**, *90*, 111.
[22] C. Kratky, H. Falk, K. Grubmayr, U. Zrunek, *Monatsh. Chem.* **1985**, *116*, 761.
[23] H. Falk, 'The Chemistry of Linear Oligopyrroles and Bile Pigments', Springer-Verlag, Wien, 1989, p. 265.
[24] J. J. P. Stewart, *J. Comp.-Aided Mol. Design* **1990**, *4*, 1.

Received February 9, 1998